NeuroImage: Clinical 14 (2017) 316–322

Contents lists available at ScienceDirect

NeuroImage: Clinical

journal homepage: www.elsevier.com/locate/ynicl

Altered structural brain changes and neurocognitive performance in pediatric HIV

Santosh K. Yadav[a,*], Rakesh K. Gupta[b], Ravindra K. Garg[c], Vimala Venkatesh[d], Pradeep K. Gupta[b], Alok K. Singh[c], Sheema Hashem[a], Asma Al-Sulaiti[a], Deepak Kaura[e], Ena Wang[a], Francesco M. Marincola[a], Mohammad Haris[a]

[a] Division of Translational Medicine, Research Branch, Sidra Medical and Research Center, Doha, Qatar
[b] Department of Radiology and Imaging, Fortis Memorial Research Institute, Gurgaon, Delhi, India
[c] Department of Neurology, King George Medical University, Lucknow, India
[d] Department of Microbiology, King George Medical University, Lucknow, India
[e] Department of Radiology, Sidra Medical and Research Center, Doha, Qatar

ARTICLE INFO

Article history:
Received 8 October 2016
Received in revised form 11 January 2017
Accepted 29 January 2017
Available online 2 February 2017

Keywords:
Human immunodeficiency virus
Cortical thickness
Subcortical volume
Structural connectivity
Neurocognitive functions
Magnetic resonance imaging

ABSTRACT

Pediatric HIV patients often suffer with neurodevelopmental delay and subsequently cognitive impairment. While tissue injury in cortical and subcortical regions in the brain of adult HIV patients has been well reported there is sparse knowledge about these changes in perinatally HIV infected pediatric patients. We analyzed cortical thickness, subcortical volume, structural connectivity, and neurocognitive functions in pediatric HIV patients and compared with those of pediatric healthy controls. With informed consent, 34 perinatally infected pediatric HIV patients and 32 age and gender matched pediatric healthy controls underwent neurocognitive assessment and brain magnetic resonance imaging (MRI) on a 3 T clinical scanner. Altered cortical thickness, subcortical volumes, and abnormal neuropsychological test scores were observed in pediatric HIV patients. The structural network connectivity analysis depicted lower connection strengths, lower clustering coefficients, and higher path length in pediatric HIV patients than healthy controls. The network betweenness and network hubs in corticolimbic regions were distorted in pediatric HIV patients. The findings suggest that altered cortical and subcortical structures and regional brain connectivity in pediatric HIV patients may contribute to deficits in their neurocognitive functions. Further, longitudinal studies are required for better understanding of the effect of HIV pathogenesis on brain structural changes throughout the brain development process under standard ART treatment.

1. Introduction

Acquired immunodeficiency syndrome (AIDS) is caused by human immunodeficiency virus (HIV) and is characterized by the progressive failure of the immune defense resulting in the life threatening complications such as infections and cancers (Frisch et al., 2000; Kumarasamy et al., 1995). The global burden of pediatric HIV remains a challenge around the world with ~3.4 millions children living with HIV (Global Burden of Disease Pediatrics Collaboration et al., 2016). Perinatal transmission of HIV is the primary source of HIV transmission in children during pregnancy, delivery and breast feeding periods. Pediatric HIV patients showed neurodevelopmental delay and subsequently cognitive impairment including visual, language, attention, memory, learning and hearing disabilities (Le Doare et al., 2012; Van Rie et al., 2008; Belman et al., 1988).

Histological studies have demonstrated tissue injury in cortical and subcortical regions in the brain of HIV patients (Kibayashi et al., 1999; Gelman, 2015; Lang et al., 1989). Magnetic resonance imaging (MRI) has been used to measure these changes *in vivo* non-invasively. Though numerous MRI studies investigated structural and functional changes in the brain of adolescent and adult HIV patients only few studies reported these changes in pediatric HIV patients (Hoare et al., 2012; Cohen et al., 2016). Previously, altered metabolites level in the brain of pediatric HIV patients is quantified using proton MR spectroscopy and correlated with $CD4^+$ counts and cognitive functions (Keller et al., 2004; Lu et al., 1996). Neuroimaging technique such as diffusion tensor imaging depicted reduced fractional anisotropy and increased mean diffusivity in multiple brain regions in pediatric HIV patients as compared to healthy controls

Abbreviations: AIDS, acquired immunodeficiency syndrome; HIV, human immunodeficiency virus; MRI, magnetic resonance imaging; ELISA, enzyme-linked immunosorbent assay; FLAIR, fluid attenuation inversion recovery; FSPGR, fast spoiled gradient echo; TR, repetition time; TE, echo time; FA, flip angel; FOV, field of view; RAKIT, revised Amsterdamse kinder intelligence; GAT, graph-theoretical analysis toolbox; ROIs, regions of interest; C, clustering coefficient; L, characteristic path length; SW, small-world index; TBM, tensor based morphometry.

* Corresponding author at: Division of Translational Medicine, Sidra Medical and Research Center, P.O. Box 26999, Doha, Qatar.
E-mail addresses: syadav@sidra.org, santoshyadav20076@gmail.com (S.K. Yadav).

http://dx.doi.org/10.1016/j.nicl.2017.01.032

(Hoare et al., 2012; Cohen et al., 2016). A recent study depicted global reduced gray matter and white matter volumes in pediatric HIV patients using volumetric based approach (Cohen et al., 2016). Since multiple cortical and subcortical brain regions are involved in the normal brain functioning and neurocognitivity by evaluating the *in vivo* changes in these structures may improve understanding of the neurobiology of pediatric HIV patients.

In the current study, we measured cortical thickness, subcortical volume, and structural connectivity in perinatally infected pediatric HIV patients and compared with those of healthy controls. Additionally, neurocognitive test scores were quantified and correlated with the brain structural changes. We hypothesized that changes in cortical thickness and subcortical volumes will affect the brain connectivity and cognitive performance in pediatric HIV patients.

2. Materials and methods

2.1. Participants

Thirty four perinatally infected pediatric HIV patients (mean ± SD, 10.2 ± 1.7 years) and 32 (mean ± SD, 11.2 ± 2.9 years) pediatric healthy controls of similar socioeconomic and ethnic group were included in this study. HIV assay was performed as per the national HIV testing protocols *i.e.* screening by HIV enzyme-linked-immunosorbent-assay (ELISA)/Rapid test followed by confirmation with 2 further HIV rapid tests of higher specificity. All subjects underwent clinical assessment including neuropsychological test and brain MRI. Informed consent was obtained from all participants or their nearest kin prior study. Institutional Ethical Committee approved the study protocol.

2.2. Magnetic resonance imaging

Brain MRI was performed on a 3 T clinical Scanner (GE Healthcare Technologies, Milwaukee, WI, United States) using a 32-channel head coil. T_2-weighted, T_1-weighted and fluid-attenuated inversion recovery (FLAIR) images were acquired to assess any gross brain pathology, such as tumor, cyst, or any other mass lesion. Presence of such anomalies and poor image quality due to motion artifacts were used as exclusion criteria. The inclusion criteria for pediatric HIV patients were infection of HIV in fetal or neonatal period and were on the antiretroviral treatment. For healthy controls, inclusion criteria were similar demographic, socioeconomic and educational status. For the structural analysis, high-resolution 3D T_1-weighted brain images were acquired using a fast spoiled gradient echo (FSPGR) BRAVO pulse sequence with following parameters: repetition time (TR) = 8.4 ms, echo time (TE) = 3.32 ms, inversion time = 400 ms, flip angel (FA) = 13°, matrix size = 512 × 512, field of view (FOV) = 240 × 240 mm^2, slice-thickness = 1.0 mm.

2.3. Neuropsychological examination

Neuropsychological examination was performed in all subjects using well-established Indian adopted Revised Amsterdamse Kinder Intelligence Test (RAKIT), which contains a battery of 9 subsets that assess language, memory, learning, visual, motor coordination, concentration, mental speed, and attention. The RAKIT test battery includes- Closure test; this is a cognition and perception test that consists of 50 presentations, Exclusion test; this cognition test consists of 50 presentations, Memory-span test; this memory test consists of 36 items, Verbal-Meaning; this is based on the knowledge of concepts and verbal conceptualization and consists of 60 items, Mazes; this is a visual-motor coordination, planning and foresight speed test and consists of 14 items, Learning-names; this memory test contains 12 items, Quantity; this is a perception based test containing 65 items, Discs; this test tells about the spatial orientation and speed of spatial visualization and it contains 18 items, hidden-figure; this test is used for the transformation of visual field and convergence/flexibility of closure and it consists of 45 items (Yadav et al., 2010).

2.4. Data processing and measurements of cortical thickness and subcortical volumes

FreeSurfer (v. 5.3.0) was used to quantify cortical thickness and subcortical volumes using high-resolution T_1-weighted images in all subjects as described in detail elsewhere (Dale et al., 1999; Fischl et al., 1999). The processed data were examined for quality and to make sure that non-brain areas were omitted from analysis. Similarly, all boundaries (gray, white, and pial) were visually evaluated, and if needed, minor edits were performed to correct the misidentified areas.

Regional changes in cortical thickness between pediatric HIV patients and healthy controls were performed on smoothed gray matter surface maps. Smoothing was performed using a Gaussian kernel (full width at half maximum, 15 mm) (Yadav et al., 2015). In the analysis, regional cortical thickness was modeled as a function of groups, and age and gender were included as covariates in the model. Monte Carlo simulations with 10,000 iterations were applied to correct for multiple comparisons using a cluster-wise threshold of $p < 0.05$. Brain sites that survived after correction for multiple comparisons are depicted on the cortical thickness maps. For structural identification, clusters with significant difference between groups were overlaid onto averaged inflated cortical surface maps.

2.5. Network analysis

2.5.1. Network construction

Graph-theoretical analysis toolbox was used for the analysis of global and regional network properties (Hosseini et al., 2012; Rubinov and Sporns, 2010). FreeSurfer parcellated 84 regions of interest (ROIs) from cortical and subcortical areas were used for the network construction. Inter-regional ROIs correlations metrics for both groups were generated using Pearson correlation coefficient.

2.5.2. Global network

To detect differences in the global network topology between groups, we measured clustering coefficient (C) and characteristic path length (L) of the network at different densities from 0.27 to 0.50 with interval of 0.02. The C and L of both groups were compared with the corresponding mean values of a random graph with the same number of nodes, total edges, and degree distribution (Sporns and Zwi, 2004; Maslov and Sneppen, 2002). The small-world index (SW) was computed as (C/Crand)/(L/Lrand), where Crand and Lrand are the mean C and L of the random network (Bassett et al., 2006). The characteristics of SW networks are: C must be significantly higher than that of cluster random networks (C/Crand ratio > 1), and L should comparable to path length of random networks (Hosseini et al., 2012) (L/Lrand ratio close to 1). We also measured the nodal characteristic (betweenness) of the structural networks at threshold density of 0.27 to detect anatomical or functional connections.

2.5.3. Network hubs

The network hub is a node with central module that has higher degree than average node and considered as a crucial regulator of effective information flow in the brain (Rubinov and Sporns, 2010). We considered a node to be a hub if its degree was higher than or equal to two standard deviations of mean network degree (Hosseini et al., 2012; Bassett et al., 2008).

2.5.4. Structural network comparison

For measuring the network difference between pediatric HIV patients and healthy controls, a non-parametric permutation test with 100 repetitions was performed. In each repetition, cortical and subcortical volumes (84 ROIs) were randomly reassigned to each individual

from the two groups and association matrices were generated for each group (Yadav et al., 2016). By thresholding the association matrices at a range of network densities, we estimated the binary adjacency matrices. The network measures were then calculated for all networks at each density. Differences in network measures between groups were calculated. The difference in network measures between groups was then placed in the corresponding permutation distribution and a two-tailed *p*-value was calculated on the basis of its percentile position (Hosseini et al., 2012; Bernhardt et al., 2011). Overall, correlation strength differences were determined by using a two-tailed sample *t*-test after performing a Fisher r-to-z transformation. FDR correction was also performed with a threshold set at $p \leq 0.05$.

3. Statistical analysis

All the statistical computations were performed using the Statistical Package for Social Sciences (SPSS) version 16.0 (SPSS Inc., Chicago, USA). Demographic, neurocognitive performance and subcortical volumes were assessed by independent student samples *t*-tests and Chi-square test. Pearson's correlation and linear regression were performed to evaluate any association among imaging parameters, neuropsychological performance, $CD4^+$ counts, age and gender and corrected for the multiple comparisons using Bonferroni correction. A *p* value ≤0.05 was considered to be statistically significant.

4. Results

4.1. Demographics and clinical characteristics

Demographic and clinical characteristics are shown in Table 1. No significant difference for age ($p = 0.12$) and gender ($p = 0.69$) was observed between pediatric HIV patients and healthy controls. All pediatric HIV patients were treated with standard cART regimen under the national pediatric HIV program.

4.2. Cortical thickness and subcortical volumes changes in pediatric HIV patients

Significantly lower cortical thickness in the left postcentral, right superior temporal and right post central regions, and significantly higher cortical thickness in the left rostral middle frontal and right rostral anterior cingulate were observed in pediatric HIV patients than those of healthy controls (Fig. 1, Table 2). No significant change in the global cortical thickness in pediatric HIV patients was observed as compared to healthy controls (Table 3).

Pediatric HIV patients showed significantly lower subcortical volumes in left and right hippocampus, anterior and mid posterior corpus callosum, and significantly higher subcortical volumes in left and right nucleus accumbens than those of healthy controls (Table 3). No appreciable change in the global subcortical volume in pediatric HIV patients was observed as compared to healthy controls (Table 3).

Table 1
Demographic and clinical variables of pediatric HIV patients and healthy controls.

Demographic and clinical variables	HIV patients ($n = 34$)	Healthy controls ($n = 32$)	*p* Value
Age (years)	10.2 ± 1.7	11.2 ± 2.9	0.12
Male/female	21/13	17/15	0.69
Education (years)	3.93 ± 2.70	3.42 ± 2.19	0.54
Ethnicity	Asian Indian	Asian Indian	NA
Peak HIV viral load (log copy/ml)	3.80 ± 1.219	–	NA
$CD4^+$ T-cell count at the time of MRI ($\times 10^6$ / L)	483 ± 240	–	NA

4.3. Global topology of cortical and subcortical structural networks

The structural networks in both pediatric HIV patients and healthy controls showed widespread positive and negative inter-regional ROIs correlations between homologous (left and right) regions. The inter-regional mean ROIs correlation networks in HIV patients (0.17 ± 0.08) showed insignificant lower correlation strength than (0.19 ± 0.07) healthy controls ($p > 0.22$).

Across a range of network densities, the structural networks depicted lower gamma (control, 1.61; HIV, 1.43), and sigma (control, 1.49; HIV, 1.34) and higher lambda (control, 1.08; HIV, 1.07) values in HIV patients than healthy controls. In both groups, the normalized clustering coefficients (gamma) were >1 and the normalized path lengths (lambda) were close to 1. The cortical and subcortical correlation networks in both groups followed a small-worldness across a wide range of densities.

4.4. Group analyses on regional network measures

Pediatric HIV patients showed significantly lower nodal betweenness in the left hippocampus (control, 2.93; HIV, 0.18; $p = 0.05$), left frontal pole (control, 0.81; HIV, 0.0; $p = 0.04$), right caudal middle frontal (control, 3.62; HIV, 0.85; $p = 0.02$), and right posterior cingulate (control, 2.00; HIV, 0.23; $p = 0.01$), and significantly higher nodal betweenness in the right thalamus (control, 0.38; HIV, 3.02; $p = 0.03$), left fusiform (control, 1.65; HIV, 6.44; $p = 0.001$), left isthmus cingulate (control, 0.005; HIV, 2.02; $p = 0.03$) and left precuneus (control, 0.80; HIV, 3.49; $p = 0.001$) than those of healthy controls.

4.5. Network hubs

On the basis of nodal betweenness network hubs were identified in the left hippocampus, left paracentral, left superiorfrontal and right caudalmiddlefrontal areas in healthy controls, while in HIV patients network hubs were in the left fusiform and left precuneus (Fig. 2).

4.6. Neuropsychological findings in pediatric healthy controls and HIV patients

Pediatric HIV patients showed significantly lower neuropsychological test scores in closure ($p = 0.003$), memory ($p = 0.01$), learning name ($p = 0.003$), and quantity ($p = 0.02$) than healthy controls. The neuropsychological test scores in exclusion ($p = 0.06$), verbal learning ($p = 0.32$), mazes ($p = 0.58$), and discs ($p = 0.44$) were insignificantly lower in pediatric HIV patients than healthy controls (Fig. 3).

4.7. Correlation of cortical and subcortical changes with CD4 +, neuropsychological profiles, age and gender

No significant correlation of $CD4^+$ count with cortical thickness and subcortical volumes was observed. The anterior corpus callosum volume showed significant positive correlation with neuropsychological test scores in discs ($r = 0.511$, $p = 0.002$) and hidden figures ($r = 0.49$; $p = 0.003$). No significant correlation between MRI markers (cortical thickness and subcortical volumes) and age was observed in pediatric HIV patients, however, healthy controls showed significant positive correlation of age with corpus callosum mid posterior ($r = 0.51$, $p = 0.003$). On combining both group, significant positive correlation of age was observed with right hippocampus (0.368, $p = 0.002$) and corpus callosum mid posterior ($r = 0.392$, $p = 0.001$), while significant negative correlation of age was observed with right rostral anterior cingulate ($r = -0.430$, $p = 0.001$) and right accumbens area ($r = -0.356$, $p = 0.003$). No gender based change in either cortical thickness or subcortical volumes was observed in any of the group.

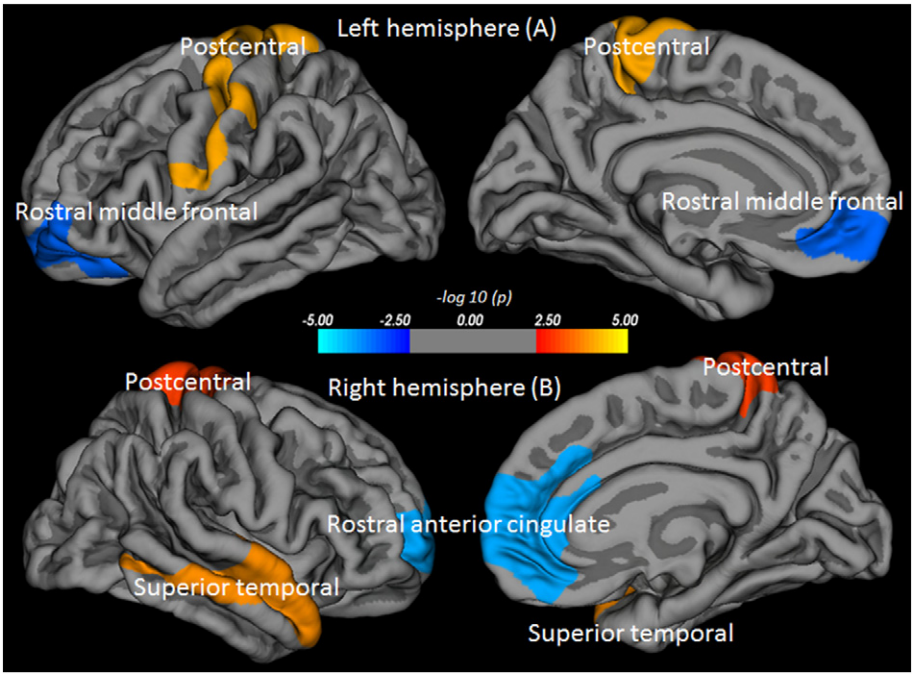

Fig. 1. Cortical thickness clusters showing significant change (Cluster wise corrected: $p < 0.05$) between pediatric HIV patients and healthy controls are projected onto the pial surface in left (A) and right (B) hemispheres respectively.

5. Discussion

Pediatric HIV patients showed altered cortical thickness, subcortical volumes, and abnormal neuropsychological test scores. The graph theory based network analysis depicted lower connection strengths, lower clustering coefficients, and higher path length in pediatric HIV patients. Moreover, pediatric HIV patients showed altered network betweenness and hubs in cortico-limbic regions.

5.1. Cortical and sub-cortical structural changes in pediatric HIV patients

Changes in the gray matter tissue density, cortical thickness, subcortical volume, white matter structures and altered brain metabolites have been previously reported in adolescent and adult HIV patients (Hoare et al., 2012; Keller et al., 2004; Cohen et al., 2010a; Cohen et al., 2010b; Sarma et al., 2014; Thompson et al., 2005; Kuper et al., 2011). Several studies using tensor based morphometry and 3D surface morphometry have shown white matter fibers damage, cortical thinning, subcortical atrophy and ventricular expansion (Chiang et al., 2007; Thompson et al., 2006; Lepore et al., 2008) in multiple brain sites in adult HIV patients. Studies using the whole brain morphometry showed decreased and increased gray matter and decreased white matter volume both in adolescent and adult HIV patients compared with healthy controls (Sarma et al., 2014; Li et al., 2014). It has been suggested that altered cortical thickness and subcortical volumes in HIV patients are due to neuronal and glial cells injury resulting from toxicity of HIV viral proteins and proinflammatory process (Nath, 2002; Zhang et al., 2003; Ben Haij et al., 2015). Briefly, HIV enters the brain within 2 weeks of infection (Williams et al., 2012) and damages neuronal and glial cells by activating the immune cells and leads to cell death along with diffuse white matter damage, breakdown of blood brain barriers and neuroinflammation (Zhang et al., 2003; Ben Haij et al., 2015; Williams et al., 2012). The pathological characteristic of HIV infected brain is the development of multinucleated giant cells and infiltration of activated immune cells such as lymphocytes, astrocytes and microglia/macrophages (Nath, 2002; Zhang et al., 2003; Budka et al., 1987; Lawrence and Major, 2002; Bell, 2004). These cells induce myelin and axonal damage, and ultimately neuronal apoptosis (Ozdener, 2005). We suggest that these pathological changes may account for reduced cortical thickness and subcortical volume in pediatric HIV patients as observed in the current study.

The current study also observed higher cortical thickness and subcortical volume in few brain areas in pediatric HIV patients as compared to healthy controls, which is consistent with the previous studies on adult HIV patients showing subcortical hypertrophy in the multiple brain sites (Castelo et al., 2007; Clark et al., 2015). Although, the exact pathophysiology for hypertrophy is not well known, we suggest that it could be related with stress-induced hypertrophy of medium spiny neurons. It is well reported that chronic stress causes hypertrophy of the dendritic trees and increases spine densities in the core division of the nucleus accumbens (Bessa et al., 2013). Chronic stress also induces dendritic hypertrophy in the corticolimbic structures implicated in the

Table 2
Brain regions showing significant change in the cortical thickness in between pediatric HIV patients and healthy controls.

Cortical regions	Max t-statistic	Size (mm^2)	TalX	TalY	TalZ	Thickness (mm), mean ± SD		*p* Values
						HIV	Controls	
Left postcentral	4.00	4093	−21	−38.8	68.6	1.86 ± 0.16	1.96 ± 0.24	0.041
Left rostral middle frontal	−3.22	2591	−38.1	50	−3.4	2.39 ± 0.23	2.23 ± 0.22	0.005
Right-rostral-anterior-cingulate	−4.00	3870	37	−3.9	14	2.74 ± 0.36	2.47 ± 0.32	0.002
Right superior temporal	3.69	3040	47.5	5	−27.2	2.97 ± 0.45	3.26 ± 0.39	0.009
Right postcentral	2.75	2279	30	−31.5	68.8	1.83 ± 0.19	2.04 ± 0.24	0.001

The magnitude of the peak (t statistic) in each area and its Tailarach coordinates (TalX, TalY and TalZ, standardized common brain space) are listed, together with the size (in normalized space) and cortical thickness (mean ± SD) for pediatric HIV patients and healthy controls.

Table 3
Brain structural changes between pediatric HIV patients and healthy controls.

Brain regions	Values (mean ± SD)		*p* Values
	HIV patients	Healthy controls	
Global cortical thickness (mm)	2.49 ± 0.10	2.52 ± 0.10	0.40
Global cortical gray matter volume (cm^3)	615.5 ± 58.9	628.0 ± 70.5	0.50
Global subcortical gray matter volume (cm^3)	53.3 ± 4.5	54.0 ± 5.8	0.32
White matter volume (cm^3)	338.1 ± 45.1	350.1 ± 45.1	0.18
Cerebrospinal fluid (cm^3)	0.70 ± 0.16	0.68 ± 0.17	0.58
Left hippocampus (cm^3)	3.57 ± 0.35	3.77 ± 0.44	0.04
Right hippocampus (cm^3)	3.58 ± 0.34	3.81 ± 0.36	0.01
Left accumbens (cm^3)	0.60 ± 0.12	0.53 ± 0.10	0.009
Right accumbens (cm^3)	0.61 ± 0.11	0.55 ± 0.11	0.03
Anterior corpus callosum (cm^3)	0.66 ± 0.12	0.72 ± 0.12	0.04
Mid posterior corpus callosum (cm^3)	0.31 ± 0.08	0.37 ± 0.07	0.01

regulation of mood. Further, it affects amygdala (Vyas et al., 2003), striatum and frontal cortex (Dias-Ferreira et al., 2009) and increases dendritic spine density and functional excitatory synaptic plasticity in nucleus accumbens (Christoffel et al., 2011).

Absence of significant correlation of age with cortical and subcortical volumes suggests the compromised neurodevelopment in pediatric HIV patients compared to healthy controls. Since we considered age and gender as a covariates in the analysis we do not expect any impact of age and gender on cortical and sub-cortical analysis in comparative analysis between pediatric HIV patients *vs* healthy controls.

5.2. Structural network changes in pediatric HIV patients

Alteration in cortical thickness and subcortical volumes are indicative of disruption of cortical and subcortical networks. Structural networks of both groups showed small-world topology, which is consistent with the previous finidngs on different human pathologies including Alzheimer's disease, schizophrenia and acute lymphoblastic leukemia (Hosseini et al., 2012; Bassett et al., 2008; Bernhardt et al., 2011; He et al., 2009; van den Heuvel et al., 2010; Yao et al., 2010). No significant difference in normalized clustering coefficient, normalized path length, and smallworld index between pediatric HIV patients and healthy controls was observed. This may be due to insignificant change in the global cortical thickness and subcortical volume (Table 3) between pediatric HIV patients and healthy controls.

In the current study, altered nodal betweenness in pediatric HIV patients was observed. A node with high betweenness can control information flow because it is at the intersection of many short paths (Sporns, 2011). In addition, a node with high betweenness in a structural network has potential to participate in large number of functional interactions (Sporns, 2011). Hippocampus and cingulate are part of the limbic system and injury in this brain site may yield the characteristic state of deficits in memory storage, while frontal pole is involved in monitoring the expected outcomes, and thalamus controls consciousness, sleep, and sensory interpretation. Altered betweenness in precuneus may have impact on memory and visuospatial functions, while altered betweenness in fusiform play a role in word recognition processing of information. Altered betweenness in these brain structures including cortico-limbic connections may responsible for the abnormal cognitive performance in pediatric HIV patients.

On the basis of nodal betweenness, we observed network hubs in the left hippocampus, left paracentral, left superiorfrontal and right caudalmiddlefrontal in healthy controls and these findings are in line with the previous study (Ajilore et al., 2014). On the other hand pediatric HIV patients showed hubs in left fusiform and left precuneus. We suggest that altered location of hubs in pediatric HIV patients might be due to injury in cortical and subcortical structures.

5.3. Neurocognitive changes in pediatric HIV patients

We observed significant lower cognitive performance in pediatric HIV patients than healthy controls, suggesting abnormal cognitive functions in pediatric HIV patients, and is in consistent with the previous findings (Malee et al., 2011).

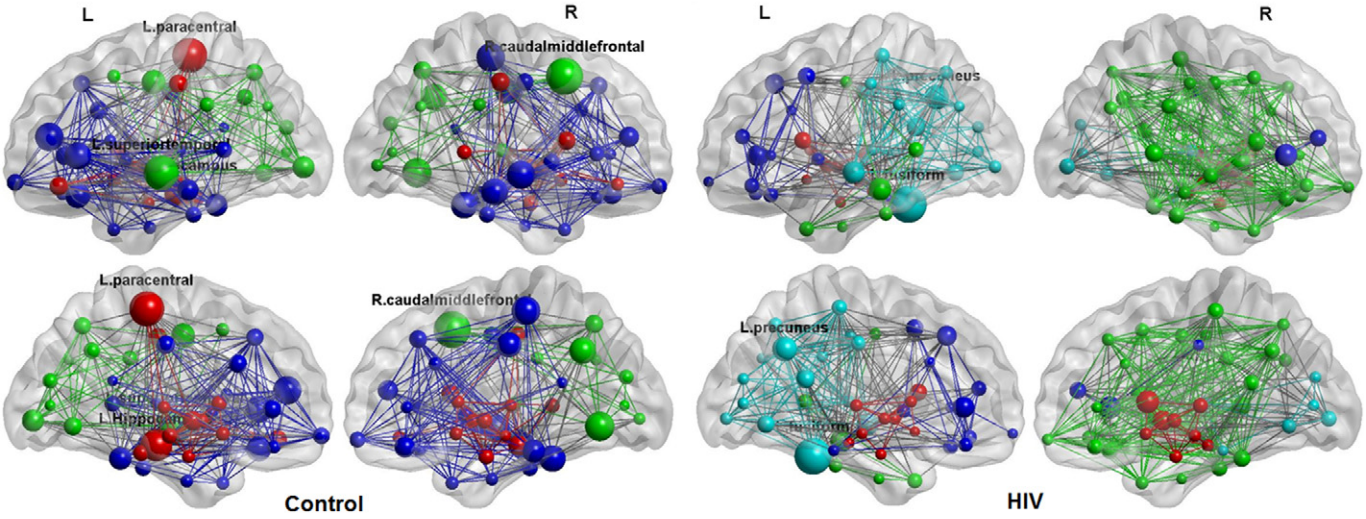

Fig. 2. Structural correlation networks and network hubs overlaid on ICBM152 brain template of pediatric HIV patients and healthy controls. Colour lines indicate connections (edge), and spheres represent regions (node). The radius of the spheres is proportional to the nodal betweenness.

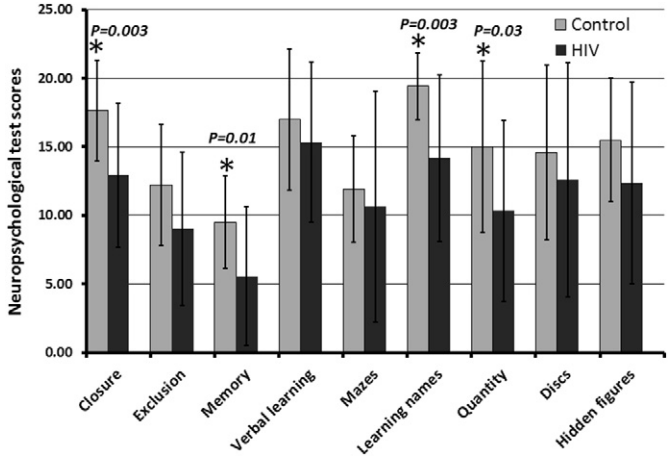

Fig. 3. Bar plots show the neuropsychological test scores (mean ± SD) in pediatric healthy controls and HIV patients. * indicates significant difference in the neuropsychological test scores between pediatric healthy controls and HIV patients.

6. Conclusions

Altered cortical thickness, subcortical volumes, regional connectivity, and neurocognitive deficits were observed in pediatric HIV patients. Presence of altered cortical thickness, subcortical volumes, and reduced regional brain connectivity may contribute to deficits in neurocognitive functions in pediatric HIV patients. Further, longitudinal studies are required for better understanding of the effect of HIV pathogenesis on brain structural changes throughout the brain development process under standard ART treatment.

Compliance with ethical standards

Funding

This study was funded by Department of Science and Technology (Grant number: SR/CSI/02/2 0 10, G).

Conflict of interest

All listed authors declare no conflict of interest.

Ethical approval

All procedures performed in this study involving human participants were in accordance with the ethical standards of the institutional and/or national research committee and with the 1964 Helsinki declaration and its later amendments or comparable ethical standards.

Informed consent

Informed consent was obtained from all individual participants included in the study.

References

Ajilore, O., Lamar, M., Leow, A., Zhang, A., Yang, S., et al., 2014. Graph theory analysis of cortical-subcortical networks in late-life depression. Am. J. Geriatr. Psychiatry 22, 195–206.

Bassett, D.S., Meyer-Lindenberg, A., Achard, S., Duke, T., Bullmore, E., 2006. Adaptive reconfiguration of fractal small-world human brain functional networks. Proc. Natl. Acad. Sci. U. S. A. 103, 19518–19523.

Bassett, D.S., Bullmore, E., Verchinski, B.A., Mattay, V.S., Weinberger, D.R., et al., 2008. Hierarchical organization of human cortical networks in health and schizophrenia. J. Neurosci. 28, 9239–9248.

Bell, J.E., 2004. An update on the neuropathology of HIV in the HAART era. Histopathology 45, 549–559.

Belman, A.L., Diamond, G., Dickson, D., Horoupian, D., Llena, J., et al., 1988. Pediatric acquired immunodeficiency syndrome. Neurologic syndromes. Am. J. Dis. Child. 142, 29–35.

Ben Haij, N., Planes, R., Leghmari, K., Serrero, M., Delobel, P., et al., 2015. HIV-1 tat protein induces production of proinflammatory cytokines by human dendritic cells and monocytes/macrophages through engagement of TLR4-MD2-CD14 complex and activation of NF-kappaB pathway. PLoS One 10, e0129425.

Bernhardt, B.C., Chen, Z., He, Y., Evans, A.C., Bernasconi, N., 2011. Graph-theoretical analysis reveals disrupted small-world organization of cortical thickness correlation networks in temporal lobe epilepsy. Cereb. Cortex 21, 2147–2157.

Bessa, J.M., Morais, M., Marques, F., Pinto, L., Palha, J.A., et al., 2013. Stress-induced anhedonia is associated with hypertrophy of medium spiny neurons of the nucleus accumbens. Transl. Psychiatry 3, e266.

Budka, H., Costanzi, G., Cristina, S., Lechi, A., Parravicini, C., et al., 1987. Brain pathology induced by infection with the human immunodeficiency virus (HIV). A histological, immunocytochemical, and electron microscopical study of 100 autopsy cases. Acta Neuropathol. 75, 185–198.

Castelo, J.M., Courtney, M.G., Melrose, R.J., Stern, C.E., 2007. Putamen hypertrophy in nondemented patients with human immunodeficiency virus infection and cognitive compromise. Arch. Neurol. 64, 1275–1280.

Chiang, M.C., Dutton, R.A., Hayashi, K.M., Lopez, O.L., Aizenstein, H.J., et al., 2007. 3D pattern of brain atrophy in HIV/AIDS visualized using tensor-based morphometry. NeuroImage 34, 44–60.

Christoffel, D.J., Golden, S.A., Dumitriu, D., Robison, A.J., Janssen, W.G., et al., 2011. IkappaB kinase regulates social defeat stress-induced synaptic and behavioral plasticity. J. Neurosci. 31, 314–321.

Clark, U.S., Walker, K.A., Cohen, R.A., Devlin, K.N., Folkers, A.M., et al., 2015. Facial emotion recognition impairments are associated with brain volume abnormalities in individuals with HIV. Neuropsychologia 70, 263–271.

Cohen, R.A., Harezlak, J., Gongvatana, A., Buchthal, S., Schifitto, G., et al., 2010a. Cerebral metabolite abnormalities in human immunodeficiency virus are associated with cortical and subcortical volumes. J. Neurovirol. 16, 435–444.

Cohen, R.A., Harezlak, J., Schifitto, G., Hana, G., Clark, U., et al., 2010b. Effects of nadir CD4 count and duration of human immunodeficiency virus infection on brain volumes in the highly active antiretroviral therapy era. J. Neurovirol. 16, 25–32.

Cohen, S., Caan, M.W., Mutsaerts, H.J., Scherpbier, H.J., Kuijpers, T.W., et al., 2016. Cerebral injury in perinatally HIV-infected children compared to matched healthy controls. Neurology 86, 19–27.

Dale, A.M., Fischl, B., Sereno, M.I., 1999. Cortical surface-based analysis. I. Segmentation and surface reconstruction. Neuroimage 9, 179–194.

Dias-Ferreira, E., Sousa, J.C., Melo, I., Morgado, P., Mesquita, A.R., et al., 2009. Chronic stress causes frontostriatal reorganization and affects decision-making. Science 325, 621–625.

Fischl, B., Sereno, M.I., Dale, A.M., 1999. Cortical surface-based analysis. II: inflation, flattening, and a surface-based coordinate system. NeuroImage 9, 195–207.

Frisch, M., Biggar, R.J., Goedert, J.J., 2000. Human papillomavirus-associated cancers in patients with human immunodeficiency virus infection and acquired immunodeficiency syndrome. J. Natl. Cancer Inst. 92, 1500–1510.

Gelman, B.B., 2015. Neuropathology of HAND with suppressive antiretroviral therapy: encephalitis and neurodegeneration reconsidered. Curr. HIV/AIDS Rep. 12, 272–279.

Global Burden of Disease Pediatrics CollaborationKyu, H.H., Pinho, C., Wagner, J.A., Brown, J.C., et al., 2016. Global and national burden of diseases and injuries among children and adolescents between 1990 and 2013: findings from the global burden of disease 2013 study. JAMA Pediatr. 170, 267–287.

He, Y., Dagher, A., Chen, Z., Charil, A., Zijdenbos, A., et al., 2009. Impaired small-world efficiency in structural cortical networks in multiple sclerosis associated with white matter lesion load. Brain 132, 3366–3379.

Hoare, J., Fouche, J.P., Spottiswoode, B., Donald, K., Philipps, N., et al., 2012. A diffusion tensor imaging and neurocognitive study of HIV-positive children who are HAART-naive "slow progressors". J Neurovirol 18, 205–212.

Hosseini, S.M., Hoeft, F., Kesler, S.R., 2012. GAT: a graph-theoretical analysis toolbox for analyzing between-group differences in large-scale structural and functional brain networks. PLoS One 7, e40709.

Keller, M.A., Venkatraman, T.N., Thomas, A., Deveikis, A., LoPresti, C., et al., 2004. Altered neurometabolite development in HIV-infected children: correlation with neuropsychological tests. Neurology 62, 1810–1817.

Kibayashi, K., Ng'walali, P.M., Mbonde, M.P., Makata, A.M., Mwakagile, D., et al., 1999. Neuropathology of human immunodeficiency virus 1 infection. Significance of studying in forensic autopsy cases at Dar es Salaam, Tanzania. Arch. Pathol. Lab. Med. 123, 519–523.

Kumarasamy, N., Solomon, S., Jayaker Paul, S.A., Venilla, R., Amalraj, R.E., 1995. Spectrum of opportunistic infections among AIDS patients in Tamil Nadu, India. Int. J. STD AIDS 6, 447–449.

Kuper, M., Rabe, K., Esser, S., Gizewski, E.R., Husstedt, I.W., et al., 2011. Structural gray and white matter changes in patients with HIV. J. Neurol. 258, 1066–1075.

Lang, W., Miklossy, J., Deruaz, J.P., Pizzolato, G.P., Probst, A., et al., 1989. Neuropathology of the acquired immune deficiency syndrome (AIDS): a report of 135 consecutive autopsy cases from Switzerland. Acta Neuropathol. 77, 379–390.

Lawrence, D.M., Major, E.O., 2002. HIV-1 and the brain: connections between HIV-1-associated dementia, neuropathology and neuroimmunology. Microbes Infect. 4, 301–308.

Le Doare, K., Bland, R., Newell, M.L., 2012. Neurodevelopment in children born to HIV-infected mothers by infection and treatment status. Pediatrics 130, e1326–e1344.

Lepore, N., Brun, C., Chou, Y.Y., Chiang, M.C., Dutton, R.A., et al., 2008. Generalized tensor-based morphometry of HIV/AIDS using multivariate statistics on deformation tensors. IEEE Trans. Med. Imaging 27, 129–141.

Li, Y., Li, H., Gao, Q., Yuan, D., Zhao, J., 2014. Structural gray matter change early in male patients with HIV. Int. J. Clin. Exp. Med. 7, 3362–3369.
Lu, D., Pavlakis, S.G., Frank, Y., Bakshi, S., Pahwa, S., et al., 1996. Proton MR spectroscopy of the basal ganglia in healthy children and children with AIDS. Radiology 199, 423–428.
Malee, K.M., Tassiopoulos, K., Huo, Y., Siberry, G., Williams, P.L., et al., 2011. Mental health functioning among children and adolescents with perinatal HIV infection and perinatal HIV exposure. AIDS Care 23, 1533–1544.
Maslov, S., Sneppen, K., 2002. Specificity and stability in topology of protein networks. Science 296, 910–913.
Nath, A., 2002. Human immunodeficiency virus (HIV) proteins in neuropathogenesis of HIV dementia. J. Infect. Dis. 186 (Suppl. 2), S193–S198.
Ozdener, H., 2005. Molecular mechanisms of HIV-1 associated neurodegeneration. J. Biosci. 30, 391–405.
Rubinov, M., Sporns, O., 2010. Complex network measures of brain connectivity: uses and interpretations. NeuroImage 52, 1059–1069.
Sarma, M.K., Nagarajan, R., Keller, M.A., Kumar, R., Nielsen-Saines, K., et al., 2014. Regional brain gray and white matter changes in perinatally HIV-infected adolescents. Neuroimage Clin. 4, 29–34.
Sporns, O., 2011. Networks of the Brain. MIT Press, Camrbridge, MA.
Sporns, O., Zwi, J.D., 2004. The small world of the cerebral cortex. Neuroinformatics 2, 145–162.
Thompson, P.M., Dutton, R.A., Hayashi, K.M., Toga, A.W., Lopez, O.L., et al., 2005. Thinning of the cerebral cortex visualized in HIV/AIDS reflects CD4+ T lymphocyte decline. Proc. Natl. Acad. Sci. U. S. A. 102, 15647–15652.
Thompson, P.M., Dutton, R.A., Hayashi, K.M., Lu, A., Lee, S.E., et al., 2006. 3D mapping of ventricular and corpus callosum abnormalities in HIV/AIDS. NeuroImage 31, 12–23.
van den Heuvel, M.P., Mandl, R.C., Stam, C.J., Kahn, R.S., Hulshoff Pol, H.E., 2010. Aberrant frontal and temporal complex network structure in schizophrenia: a graph theoretical analysis. J. Neurosci. 30, 15915–15926.
Van Rie, A., Mupuala, A., Dow, A., 2008. Impact of the HIV/AIDS epidemic on the neurodevelopment of preschool-aged children in Kinshasa, Democratic Republic of the Congo. Pediatrics 122, e123–e128.
Vyas, A., Bernal, S., Chattarji, S., 2003. Effects of chronic stress on dendritic arborization in the central and extended amygdala. Brain Res. 965, 290–294.
Williams, D.W., Eugenin, E.A., Calderon, T.M., Berman, J.W., 2012. Monocyte maturation, HIV susceptibility, and transmigration across the blood brain barrier are critical in HIV neuropathogenesis. J. Leukoc. Biol. 91, 401–415.
Yadav, S.K., Srivastava, A., Srivastava, A., Thomas, M.A., Agarwal, J., et al., 2010. Encephalopathy assessment in children with extra-hepatic portal vein obstruction with MR, psychometry and critical flicker frequency. J. Hepatol. 52, 348–354.
Yadav, S.K., Gupta, R.K., Saraswat, V.A., Rangan, M., Thomas, M.A., et al., 2015. Reduced cortical thickness in patients with acute-on-chronic liver failure due to non-alcoholic etiology. J. Transl. Med. 13, 322.
Yadav, S.K., Kathiresan, N., Mohan, S., Vasileiou, G., Singh, A., et al., 2016. Gender-based analysis of cortical thickness and structural connectivity in Parkinson's disease. J. Neurol.
Yao, Z., Zhang, Y., Lin, L., Zhou, Y., Xu, C., et al., 2010. Abnormal cortical networks in mild cognitive impairment and Alzheimer's disease. PLoS Comput. Biol. 6, e1001006.
Zhang, K., McQuibban, G.A., Silva, C., Butler, G.S., Johnston, J.B., et al., 2003. HIV-induced metalloproteinase processing of the chemokine stromal cell derived factor-1 causes neurodegeneration. Nat. Neurosci. 6, 1064–1071.